Contrib Mineral Petrol (2002) 142: 449–464
DOI 10.1007/s004100100302

B. Cesare · D. Rubatto · J. Hermann · L. Barzi

Evidence for Late Carboniferous subduction-type magmatism in mafic-ultramafic cumulates of the SW Tauern window (Eastern Alps)

Received: 14 May 2001 / Accepted: 6 August 2001 / Published online: 5 October 2001

Abstract Hectometric bodies of fresh mafic-ultramafic cumulates have been discovered within the Central Gneiss of the Zillertal massif, SW Tauern window (eastern Alps, Italy). The cumulates, intruded by the Central Gneiss granitoids, are amphibole-bearing harzburgites and norites made of cumulitic olivine ($Fo_{73–80}$), spinels, sulphides and plagioclase ($An_{79–87}$), included in orthopyroxene ($En_{76–83}$) and Ti-pargasite (Mg# = 0.73–0.81). Major and trace element geochemistry indicates that these rocks represent olivine + spinel ± plagioclase cumulates, in which interstitial melt crystallized as orthopyroxene + Ti-pargasite. The parental melt has trace element patterns typical of subduction zone magmas. The crystallization sequence, mineral compositions, and modes indicate that cumulates formed from a H_2O-rich basaltic andesite, which intruded at low-pressure (~2 kbar) and temperatures of 1,050–1,100 °C. SHRIMP U-Pb dating of zircons from ultramafic cumulates and adjacent metagranodiorite yielded ages of 309 ± 5 and 295 ± 3 Ma, respectively. In agreement with field relationships, these results show that the mafic-ultramafic cumulates represent a co-genetic, early product of the Late Carboniferous plutonic activity in the western Tauern window, which started in the Westphalian, earlier than previously thought. Our data on the most primitive rocks in the Zillertal massif permit, for the first time, insight into the parental magma and thus into the origin of this Late Carboniferous calc-alkaline magmatism, which was most likely related to slab break off during the Late Variscan convergence.

B. Cesare (✉) · L. Barzi
Dipartimento di Mineralogia e Petrologia,
Università di Padova, C.N.R. Centro di Studio
per la Geodinamica Alpina, Corso Garibaldi,
37, 35137 Padova, Italy
E-mail: bernardo@dmp.unipd.it
Tel.: +39-049-8272019
Fax: +39-049-8272010

D. Rubatto · J. Hermann
Research School of Earth Sciences,
The Australian National University,
Canberra ACT 0200, Australia

Editorial responsibility: J. Hoefs

Introduction

The Variscan magmatic rock suites of the Alpine belt are very poor in preserved primitive mafic intrusions (von Raumer 1998). Because they are much less affected by crustal processes, which blur the origin of the magmatism, primitive mafic rocks are crucial for the reconstruction of the Variscan magmatic activity and hence Variscan tectonics.

In the western Tauern window, Central Gneisses (“Zentralgneise”) consisting of tonalites, granodiorites, and granites are the most widespread rocks (e.g. Finger et al. 1993). These Variscan batholiths intruded in the paleo-European, Penninic domain, and were involved in the build-up of the Alpine chain (Morteani 1974; Lammerer and Weger 1998). The Variscan intrusives in the western Tauern window are classified as calc-alkaline I-type granitoids (Finger and Steyrer 1988; Finger et al. 1993).

In their genetic distinction of the various typologies of Variscan granitoids, Finger et al. (1997) ascribe the Central Gneisses of the western Tauern window to the post-collisional, high-level Type 4, with intrusion ages in the range 310–290 Ma. According to the same authors, most of these granitoids do not show obvious relationships to mafic melts, and hence it is difficult to gain information on their possible sources, on the involvement of mantle-derived melts, and on the tectonothermal scenario in which the magmatism originated. Mafic (metagabbros) and ultramafic (metahornblendites) rocks were reported as minor products in the Central Gneisses of the western Tauern window by Arming (1993), but his samples were completely altered to amphibolites by the Alpine metamorphism, which complicated the understanding of their genesis.

In this paper, we report for the first time the petrologic, geochemical, and geochronological features of fresh mafic-ultramafic cumulates within the Zillertal-Venediger (hereafter "Zillertal" for short) massif of the Central Gneiss. The well-preserved magmatic fabric and mineralogy of these cumulates permit postulation of a crystallization sequence and an estimate on intrusion depth. The genetic link between the cumulates and the Central Gneiss granitoids, and the relevance of the cumulates in the Variscan geologic evolution of the Penninic realm are based on age data obtained by SHRIMP U-Pb dating of magmatic zircon. The petrology and geochronology combined with the major and trace element chemical composition of the mafic-ultramafic cumulates provide an opportunity to widen the knowledge about the Variscan batholiths, and to add constraints to the geodynamic setting of the Late Carboniferous magmatism.

Geologic background

The Penninic domain of the Tauern window consists of widespread Variscan granitoids ("Central Gneiss"), and of their country rocks ranging in age from Upper Precambrian to lower Palaeozoic, lower Schieferhülle, and of their Upper Carboniferous to Mesozoic cover, upper Schieferhülle (Morteani 1974; Lammerer and Weger 1998 and references therein). During the Alpine orogeny, this basement and cover unit represented the European continental margin. It was overthrusted by both the Penninic oceanic nappes, and by the Austroalpine basement nappes, forming a nappe stack in which the Central Gneisses are the lowermost structural unit. In the western Tauern window, two large, ENE-WSW elongated Central Gneiss antiforms can be defined, which outcrop on an area of approximately 1,000 km^2 (Fig. 1): the Tux-Ahorn massif to the north, and the Zillertal massif to the south (Finger et al. 1993 and references therein).

The Zillertal Central Gneiss comprises tonalites, granodiorites and granites (Finger et al. 1993; Eichhorn et al. 2000), variably altered and deformed into gneisses ("Augen-" and "Flasergneiss", Morteani 1974) during the Alpine metamorphic cycle. These granitoids represent part of voluminous, Late Carboniferous (Stephanian) magmatic activity with a calc-alkaline, I-type affinity, dated at 292 ± 6 Ma in the eastern Venediger unit (Eichhorn et al. 2000). The prevailing rock type in the Zillertal massif is a medium-grained biotite-bearing metatonalite to metagranodiorite (De Vecchi and Mezzacasa 1986). Granites are much less common, and appear to be the youngest intrusions, cutting the tonalites. The field relationships indicate that these tonalitic-granodioritic Central Gneisses of the Zillertal intruded as high level plutons (Finger et al. 1997) after a phase of intense uplift and erosion (Eichhorn et al. 2000).

Based on new U-Pb SHRIMP zircon data and on the compilation of zircon ages by Finger et al. (1997), it has recently been proposed that in the central Tauern window the Late Carboniferous magmatism of the Central Gneiss is restricted to the interval 300–280 Ma (Eichhorn et al. 2000). In fact, a lack of geochronological data is observed in the interval 340–300 Ma. The origin of the calc-alkaline, I-type Stephanian plutons is debated. In their recent review of possible geodynamic models, Eichhorn et al. (2000) consider subduction-related processes as unlikely, and favor a combination of magmatic underplating and crustal decompression melting in a regime of lithospheric extension.

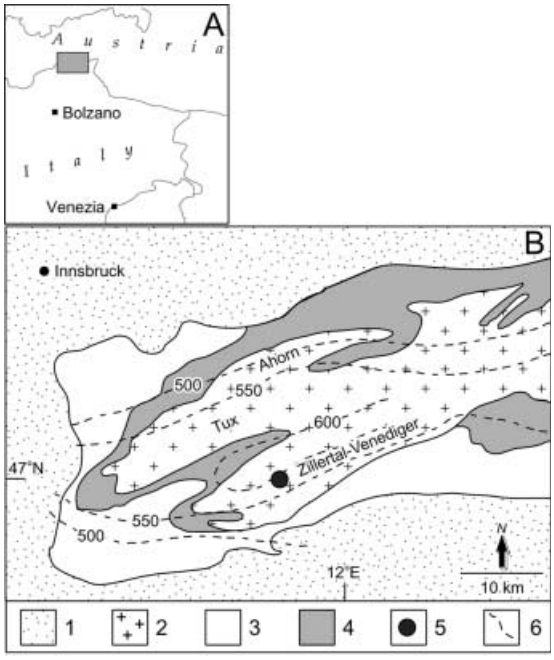

Fig. 1 **A** Location (*shaded box*), **B** schematic geologic map of the western Tauern window, modified after Selverstone (1985). *1* Austroalpine basement; *2* Central Gneiss (Zentralgneis); *3* upper Schieferhülle; *4* lower Schieferhülle; *5* location of study area; *6* isotherms of the maximum temperature during the Tauern metamorphism (from Hoernes and Friedrichsen 1974)

The studied area is located on the southern flank of the Cima di Campo (Turnerkamp)–Monte Corno (Hornspitze) ridge (Fig. 1), at the core of the western Zillertal massif. This locality is about 3 km to the north of the tectonic contact with the Paleozoic and Mesozoic sequences of the lower and upper Schieferhülle (Morteani 1974; De Vecchi and Baggio 1982; De Vecchi and Mezzacasa 1986). In this region, the structure of the Central Gneisses ranges from strongly foliated to non-deformed proceeding to the north, i.e. away from the tectonic boundary where Alpine deformation was more intense (De Vecchi and Mezzacasa 1986).

Similar to the overlying units of the Tauern window, the Central Gneisses were deeply affected by Alpine deformation and metamorphism (Morteani 1974; Raith 1971; Raith et al. 1978). This involved an early blueschist to eclogite facies event (Selverstone et al. 1984), followed by decompression to 5–7 kbar and thermal peak at 650 °C during the Oligocene "Tauern

metamorphism'' (Hoernes and Friedrichsen 1974; Friedrichsen and Morteani 1979). The maximum temperatures recorded in the studied area during the Alpine metamorphism were in the range 550–600 °C, and were attained at ~30 Ma (Christensen et al. 1994).

Morteani (1974) noted that even the isotropic rocks which retained a magmatic texture (massive metatonalites to metagranites) have undergone a complete metamorphic recrystallization during the Tauern metamorphism. This holds also for the mafic-ultramafic rocks studied by Arming (1993), which were totally transformed into amphibolites. One exception is represented by the cumulates recently found and described by Barzi (1996). Owing to the very fast retreat of Alpine glaciers in the last decade, these fresh intrusives with well-preserved magmatic associations have been exposed in scattered outcrops and are studied here.

The mafic-ultramafic cumulates

The masses of fresh cumulates crop out within the Vedretta di Dentro (Trattenbach) glacier, at an elevation of ~3,000 m, in an area mapped and investigated by Arming (1993), De Vecchi and Mezzacasa (1986) and Frasl and Schindlmayr (1995). At present, the cumulates are exposed as hectometric bodies (Fig. 2), but they are likely to be in continuity with the larger masses of Monte Corno (Hornspitze) and would thus define a 3-km-long mafic-ultramafic complex within the metatonalites-metagranodiorites.

In the field, the cumulates are often crosscut by the more acidic rocks forming the Central Gneisses, and in particular by the metatonalites. Metatonalites crosscut the cumulates along an irregular pattern of fractures, disrupting a weak layering indicative of magmatic settling (Fig. 3). The blocks of cumulates frequently show straight to slightly curved surfaces, with sharp contacts and no signs of interaction between the two lithologies. We interpret these field relationships such that the cumulates are older than, and intruded by, the metatonalites.

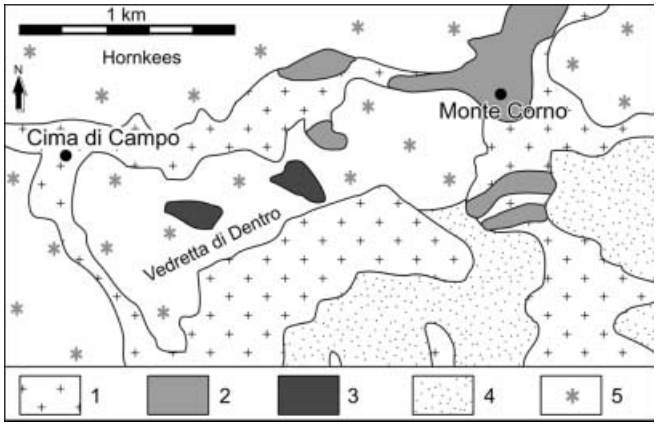

Fig. 2 Sketch map of the Cima di Campo–Monte Corno area, modified after Arming (1993) and Barzi (1996). *1* Metatonalites and metagranodiorites of the Zillertal massif; *2* amphibolites (altered mafic-ultramafic rocks); *3* fresh mafic-ultramafic cumulates; *4* debris, morain; *5* glacier

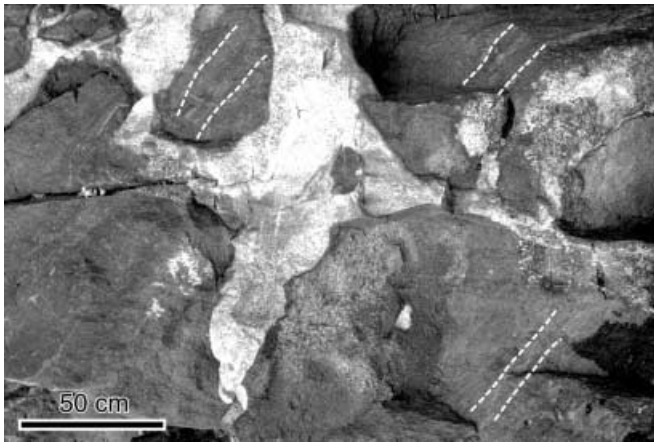

Fig. 3 Granodioritic apophysis crosscutting the mafic-ultramafic cumulates, in which a weak magmatic layering can be observed (*dashed white lines*). Disruption of the layering, and local straight edges of cumulate blocks with sharp contacts between lithologies indicate that cumulates were intruded when they were mostly solidified

The main lithologies characterizing the mafic-ultramafic complex are well-preserved amphibole-bearing peridotites and norites and their metamorphic derivatives. The mafic-ultramafic cumulates are often statically recrystallized amphibolites in which the original magmatic structure is still recognizable.

The least altered mafic-ultramafic cumulates are characterized by an inequigranular, poikilitic texture, with grain size in the range 0.5–15 mm (Fig. 4a). The magmatic mineralogical association includes olivine, plagioclase, apatite, opaque minerals (Al-chromite, magnetite and sulphides), amphibole (pargasitic hornblende), and orthopyroxene. A few samples contain primary phlogopite and zircon. Locally, a discontinuous banded structure due to alternating amphibole-rich and orthopyroxene-rich layers is observed. As the layering is not evident at a macroscopic scale, the cumulates can be classified as amphibole-bearing harzburgitic orthocumulates and amphibole-bearing noritic orthocumulates, following the terminology of Irvine (1982).

Olivine is the most abundant cumulus mineral, and occurs as rounded to subhedral crystals ranging in size from 0.5 to 2 mm (Fig. 4b). It is generally fresh, and includes primary opaques: Al-chromite (the most abundant), ilmenite, Cr-magnetite, magnetite, phyrrotite and pentlandite. When in contact with phlogopite or more rarely with amphibole, olivine may develop a corona of orthopyroxene.

Plagioclase is a cumulus phase, which occurs as two generations: most commonly as euhedral laths <0.5 mm, more rarely as crystals >1 mm, or polycrystalline clusters up to 1 cm across. Plagioclase does not include primary oxides or sulphides. Overall, the cumulus minerals constitute 40 to 80 vol% of the rocks.

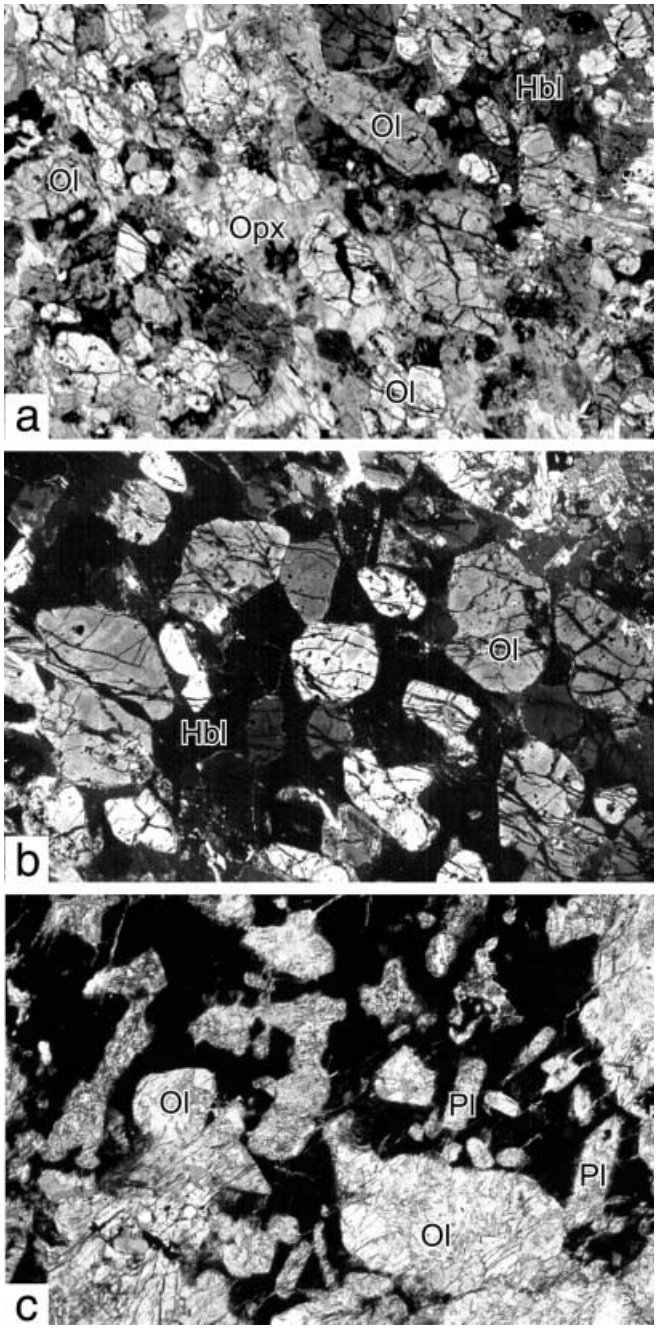

Fig. 4 **a** Typical microstructure of a plagioclase-poor ultramafic cumulate, with olivine (*Ol*) included in poikilitic pargasitic hornblende (*Hbl*, *top right*) or orthopyroxene (*Opx*, *top left*). Crossed polars, width of view = 20 mm. **b** Subhedral to rounded crystals of olivine included in intercumulus pargasitic hornblende. Crossed polars, width of view = 3.5 mm. **c** Preserved primary cumulitic microstructure in completely transformed Alpine amphibolites. The *black background* is an aggregate of green hornblende and ilmenite needles pseudomorphing magmatic pargasitic hornblende. Sites of plagioclase laths (*Pl*) and olivine crystals (*Ol*) can still be recognized. Plane-polarised light, width of view = 13 mm

The magmatic amphibole is a pargasitic hornblende with marked pleochroism to brown-orange, grain size generally >5 mm, and anhedral shape. Along with olivine, plagioclase and opaques, it may include euhedral crystals of orthopyroxene. These microstructures suggest that hornblende was the last crystallizing phase.

Orthopyroxene is less abundant than amphibole and forms subhedral intercumulus crystals ranging in grain size from 0.5 to 8 mm, generally >5 mm, and includes olivine, plagioclase, and opaques. It shows a marked pleochroism, in places with patchy distribution, and local undulose extinction and microfracturing, which testify for slight post-magmatic deformation.

The microstructural analysis, based on appearance and mutual inclusion relationships, indicates that plagioclase and olivine are cumulus phases whereas orthopyroxene and pargasitic amphibole represent intercumulus phases. The observation that Cr-spinel and Ni-sulphides are generally only found as inclusions in olivine suggests that they crystallized early. The high amount of cumulus olivine, and the fact that oxides are never found in plagioclase indicates that olivine started to crystallize prior to plagioclase. In summary, the following crystallization sequence for both harzburgites and norites can be postulated: Cr-spinel ± Ni-sulphides >olivine >plagioclase >orthopyroxene >pargasite.

During the Alpine polymetamorphic cycle, alteration of cumulates generally took place without deformation, ranging from limited coronitic alteration of olivine and plagioclase, to complete amphibolitization. In the latter case, the metamorphic paragenesis consists essentially of Mg-hornblende, chlorite, andesine, and biotite. Despite complete mineralogical renewal, the primary cumulitic structure is evident in the arrangement of Ti-oxides that mimic the distribution of former pargasitic hornblende and its poikilitic texture (Fig. 4c).

Analytical methods

Whole-rock major and trace element compositions were determined with X-ray fluorescence (XRF) with the Philips PW 2400 spectrometer of the Centro di Studio per la Geodinamica Alpina (CSGA–CNR, Padova).

The major-element mineral compositions were analyzed with electron microprobe (EMP) with a CAMECA Camebax (CSGA–CNR, Padova), using an accelerating potential of 15 kV, beam current of 15 nA, counting times of 10 s, natural and synthetic mineral standards, and a focused beam of ~1-μm diameter. Matrix effects were corrected by a ZAF method. Ni in olivine was determined by wave dispersive spectrometry (WDS) using an acceleration voltage of 25 kV and a beam current of 30 nA with a CAMECA Camebax microprobe at the Research School of Earth Sciences (RSES).

Whole-rock rare earth element (REE) compositions were determined from glasses obtained from rock powders by Laser Ablation-ICP-MS analysis at the (RSES), Canberra. LA-ICP-MS analyses (Eggins et al. 1998) used a pulsed 193 nm ArF Excimer laser with 100 mJ energy at a repetition rate of 5 Hz. A mixed He-Ar stream transported the aerosol into the ICP-MS (Agilent 7500). Detection limits were ≤0.01 ppm for a 170-μm-diameter pit.

Zircon was prepared as mineral separate, mounted in epoxy and polished down to expose the grain centers. The selection of zircons for U-Pb analyses based on the cathodoluminescence images. Cathodoluminescence investigation was carried out at the Electron Microscope Unit at the Australian National University on a HITACHI S2250-N scanning electron microscope working at 15 kV, ~60 μA and ~20 mm working distance. Zircon was analyzed for U, Th, and Pb using the sensitive high-resolution ion microprobe (SHRIMP II) at the RSES. Instrumental conditions and data acquisition for zircon were generally as described by Compston et al. (1992). The data were collected in sets of six to seven scans throughout the nine masses and a reference zircon was analyzed each fourth analysis. The measured $^{206}Pb/^{238}U$ ratio was corrected using reference zircon from a gabbro of the Duluth Complex in Minnesota (AS3, 1,099 Ma). The data were corrected for common Pb on the basis of the measured ^{204}Pb and assuming a Broken Hill common lead composition, which approximates the laboratory common lead at RSES. Ages were calculated using the Isoplot/Ex program of Ludwig (2000). Average ages are given at 95% confidence level.

Mineral chemistry

The chemical composition of minerals inferred to be most representative of the magmatic stage were analyzed by EMP on ten samples. Although Table 1 reports representative EMP analyses, the description and discussion below refer to the entire dataset.

Olivine shows a chemical zoning, with more magnesian cores (e.g. Fo_{80}) than rims (e.g. Fo_{76}; Fig. 5a). Olivine composition also varies with grain size, smaller crystals having generally lower Mg# (Mg/(Mg + Fe)), or between samples: the measured compositional range is Fo_{73}-Fo_{80}, with an average of Fo_{76}. Ca and Cr are always below detection limits. The olivines contain about 650–750 ppm Ni as determined by EMP-WDS analyses. The Mg# as well as the Ni content of olivine is significantly lower than in mantle peridotites (e.g. Ernst 1978)

Plagioclase composition is bytownitic, and clusters in the range An_{73}-An_{87} (Fig. 5b). A weak zoning, with decreasing anorthite content from core (An_{83}) to rim (An_{78}), is occasionally observed.

The compositions of coexisting olivine and plagioclase of several cumulates are shown in Fig. 5b. The high An content of plagioclase cores at an intermediate to high Mg# of olivines cores suggests that the investigated cumulates have a greater affinity to arc rocks than to tholeiitic, MORB-type cumulates.

Orthopyroxene displays the largest chemical variations, with Mg# ranging from 0.76 to 0.83, Al_2O_3 up to 3.2 wt% and CaO up to 1.3 wt%. The scatter of Mg# is primarily due to differences between the various samples, where Pl-poor cumulates commonly have the highest Mg#. Within-samples variations of Mg# are <5%.

Table 1 Representative EMP analyses of primary magmatic minerals in the fresh mafic-ultramafic cumulates. *b.d.* Below detection limits

Phase	Pl	Pl	Pl	Pl	Amp	Amp	Ol	Ol	Ol	Ol	Ol	Ol	Ol	Ol	Opx	Opx	Opx	Opx	Mag	Al-Chr
Sample	45	22	22	16	46	21	46	45	45	22	21	21	16	10	45	45	46	21	10	10
		Rim	Core	Rim	Core			Rim	Core	Core	Rim	Core								
SiO_2	46.38	47.53	46.95	47.92	47.71	43.40	44.06	38.62	38.57	38.77	38.53	37.98	39.04	38.71	38.11	55.09	54.56	54.90	56.00	b.d.	b.d.
TiO_2	b.d.	b.d.	b.d.	b.d.	b.d.	3.41	1.38	0.02	b.d.	b.d.	b.d.	b.d.	b.d.	b.d.	0.01	0.07	0.02	0.09	b.d.	0.17	2.67
Al_2O_3	34.12	33.75	33.91	33.15	33.28	11.37	12.45	b.d.	b.d.	b.d.	b.d.	b.d.	b.d.	b.d.	b.d.	2.46	2.19	1.71	0.73	b.d.	18.01
Cr_2O_3	0.02	b.d.	b.d.	0.06	b.d.	0.04	0.71	b.d.	b.d.	b.d.	b.d.	b.d.	b.d.	b.d.	b.d.	0.06	0.10	0.05	b.d.	0.55	31.48
FeO	0.05	b.d.	b.d.	0.07	0.08	9.01	7.37	22.16	21.22	19.67	21.17	23.38	19.45	22.03	23.15	13.37	14.82	13.49	12.41	30.97	32.16
Fe_2O_3																				68.06	11.76
MnO					0.08	0.20	0.20	0.22	0.29	0.20	0.27	0.25	0.29	0.22	0.25	0.32	0.29	0.33	0.30	b.d.	b.d.
MgO	0.02	b.d.	b.d.	b.d.	0.03	15.85	16.87	39.53	40.48	41.87	40.08	38.52	41.24	39.17	38.39	28.11	27.81	28.31	30.18	0.09	2.79
CaO	17.74	16.29	17.25	16.47	16.68	11.57	11.30	b.d.	b.d.	b.d.	b.d.	b.d.	0.04	b.d.	b.d.	0.67	0.35	1.06	0.46		
Na_2O	1.67	2.39	2.18	2.24	2.11	2.59	2.83									b.d.	b.d.	b.d.	b.d.		
K_2O	b.d.	b.d.	b.d.	b.d.	b.d.	0.49	0.49														
ZnO																				b.d.	0.59
NiO								0.09	0.09											0.06	b.d.
$Ni_{(ppm)}$*								745	684												
Total	100.02	99.96	100.29	99.93	99.90	97.79	97.66	100.56	100.65	100.60	100.05	100.15	100.07	100.15	99.95	100.16	100.17	99.99	100.08	99.92	99.46
An%	85	78	83	80	81																
Mg#						0.76	0.80	0.76	0.77	0.79	0.77	0.75	0.79	0.76	0.75	0.79	0.77	0.79	0.81	0.01	0.13
Ülv																				0.5	6.8
Spl																				0.0	36.0
Chr																				0.8	42.2
Mag																				98.6	15.0

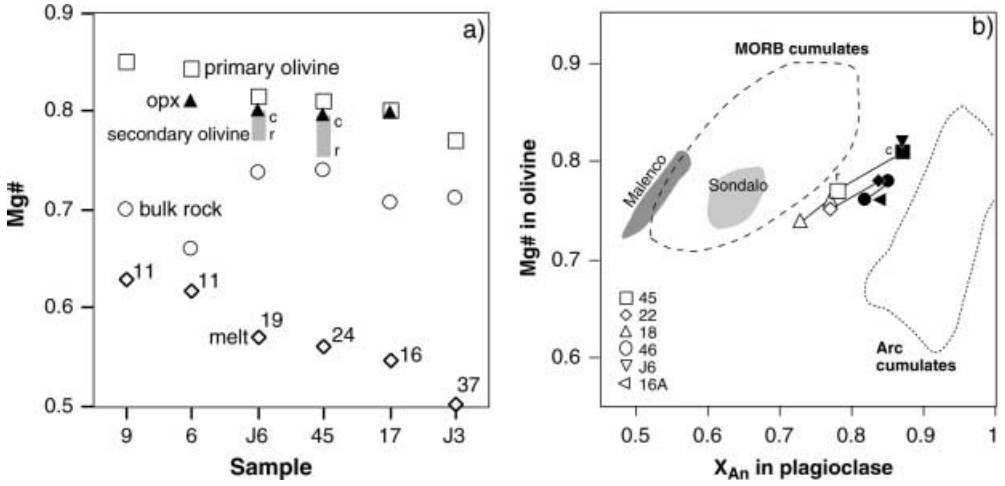

Fig. 5 **a** Measured Mg# of orthopyroxene (*filled triangles*) and olivine, core (*c*) to rim (*r*) variation (*gray bars*). The Mg# of primary olivine (*open squares*) and melt (*open diamonds*) are calculated on the basis of measured bulk rock Mg# (*open circles*) and estimated amounts of cumulus olivine and trapped melt (Table 2). The range of Mg# of original olivine (0.84–0.78) indicates that the mafic-ultramafic cumulates originate from differently evolved magmas. This is supported by the increase in calculated Yb contents (in ppm) with decreasing Mg# of the trapped melts (shown as labels on the melt symbols). **b** The compositions of coexisting olivine and plagioclase from the mafic-ultramafic cumulates. Tie-lines show the variation from core (*filled symbols*) to rim (*open symbols*) compositions. The fields for MORB-type cumulates and arc cumulates as well as the range for the Sondalo troctolites are taken from Tribuzio et al. (1999). The field for Malenco olivine gabbronorites stems from Hermann et al. (2001)

Amphibole can be defined as pargasitic hornblende (Leake 1978), with only one analysis in the field of pargasite. The TiO_2 content can be up to 4.5 wt%, and the Mg# is in the range 0.73–0.81. Again, higher Mg# values are detected in the most mafic, Pl-poor cumulates.

Opaque minerals of the magmatic assemblage include spinel (magnetite and Al-chromite), ilmenite, and sulphides. Magnetite is almost stoichiometric, Cr being the only extra component in appreciable amounts (<1.8 wt% Cr_2O_3). Al-chromite displays chemical variations in the range $Mag_{10–20}Chr_{40–45}Spl_{35–40}Ülv_{0–7}$, and ZnO up to 2 wt%. The common occurrence of ilmenite exsolution within Al-chromite suggests that the primary ülvolspinel component was higher than measured. Phyrrotite is stoichiometric FeS, whereas pentlandite contains up to 5 wt% Co.

Bulk chemistry

Major and trace element contents of six samples (6, 9, 17, 45, J3 and J6) have been determined (Table 2). All the samples display very similar features although they have different degrees of Alpine overprint. This indicates that also the samples with Alpine metamorphism can be used to constrain the magmatic evolution. Only sample 6 probably underwent minor metasomatism by Alpine fluids because of the presence of Alpine biotite, which suggests an enrichment in bulk K and other large ion lithophile elements (LILE).

Major elements

The samples display low SiO_2 contents, between 43 and 48%, and a wide range of MgO and Al_2O_3 which demonstrate that the rocks represent cumulates with various amounts of cumulus olivine and plagioclase (Fig. 5). The high Ca and Al contents as well as relatively low Mg# (Fig. 6) clearly indicate that these rocks are cumulates derived from a mafic melt, and cannot be regarded as ultramafic rocks with a mantle origin. Petrography indicates that spinel, olivine, and plagioclase are the main cumulus phases, whereas the other minerals are intercumulus phases probably originating from crystallizing interstitial trapped melt. Using the approximate composition of cumulus phases and a typical primitive mafic melt for subduction zone magmas, the proportions of olivine, plagioclase and melt can be roughly estimated from variation plots (Fig. 6; Table 2). The rocks with high MgO contents contain about 55% cumulus olivine. The Ni content of the rocks displays a positive correlation with the Mg content (Fig. 5b). This feature can be ascribed to decreasing amounts of cumulus olivine with about 750 ppm Ni. The rocks with the highest SiO_2 have the highest amount of trapped melt, whereas the high Al_2O_3 rocks are characterized by high amounts of plagioclase (up to 50%) as indicated by the largest positive Sr anomaly (Fig. 6a).

Using the measured bulk Mg# of the rocks, the experimentally determined Fe-Mg partitioning between olivine and melt (Roeder and Emslie 1970) and their estimated proportions (Table 2), the primary Mg# of cumulus olivine and melt can be back-calculated (Fig. 5a): the most primitive olivines had a Mg# of ~0.84, and the more evolved rocks had olivines with Mg# of 0.81 to 0.77. The actually measured Mg# of 0.73–0.80 in olivines is lower than the back-calculated

Table 2 Bulk rock composition of the mafic-ultramafic cumulates. The proportions of cumulus olivine, plagioclase and interstitial melt are estimated from Fig. 5. Due to uncertainties in end-member compositions, an absolute error of ±5% must be considered for the estimated proportions

Sample	45	17	9	6	J6	J3
Major elements (XRF)						
SiO_2	43.05	44.74	46.27	47.75	43.06	43.20
TiO_2	0.33	0.21	0.49	0.59	0.35	0.29
Al_2O_3	12.06	17.26	9.71	17.56	10.14	17.67
Fe_2O_3	11.99	10.04	12.02	9.32	13.54	9.69
MnO	0.15	0.12	0.17	0.12	0.17	0.11
MgO	21.41	15.42	17.64	11.38	24.21	15.10
CaO	6.49	8.49	7.91	8.47	5.14	8.18
Na_2O	1.30	1.28	0.96	1.81	1.08	1.61
K_2O	0.49	0.31	0.47	0.64	0.34	0.39
P_2O_5	0.06	0.05	0.08	0.09	0.07	0.06
LOI	2.67	2.34	3.66	2.44	1.83	4.05
Total	100.00	100.27	99.38	100.17	99.93	100.35
Estimated proportions						
Olivine	50	35	30	15	55	35
Plagio-clase	30	45	5	20	20	55
Melt	20	20	65	65	25	10
Trace elements in ppm (XRF)						
F	404	357	321	312	436	436
Sc	21	29	26	27	18	28
V	59	31	98	108	70	46
Cr	1,609	813	1,796	653	2,038	818
Co	117	82	92	60	137	82
Ni	487	311	417	198	553	312
Cu	87	55	90	55	107	53
Zn	136	79	89	92	97	83
Ga	9	11	8	13	8	11
Trace elements in ppm (LA-ICPMS)						
Rb	13.9	8.5	12.9	17.6	8.6	13.1
Sr	202	298	70	341	163	455
Y	7.60	4.75	11.25	11.98	7.32	5.96
Zr	41.9	31.9	50.1	68.9	38.5	36.8
Nb	2.81	2.06	3.13	4.84	2.23	2.35
Cs	1.41	1.66	1.47	1.67	0.98	1.92
Ba	125	97	116	219	91	103
La	6.63	5.33	7.76	10.21	5.82	6.78
Ce	13.5	10.2	16.3	21.6	12.1	13.4
Pr	1.63	1.19	2.08	2.74	1.49	1.58
Nd	6.74	4.74	9.10	11.69	6.31	6.27
Sm	1.48	0.95	2.12	2.57	1.36	1.25
Eu	0.52	0.41	0.64	0.81	0.46	0.48
Gd	1.45	0.91	2.19	2.49	1.39	1.18
Tb	0.22	0.14	0.34	0.37	0.21	0.18
Dy	1.44	0.88	2.19	2.35	1.39	1.12
Ho	0.29	0.18	0.44	0.46	0.28	0.23
Er	0.84	0.53	1.24	1.29	0.83	0.65
Tm	0.12	0.08	0.18	0.19	0.12	0.09
Yb	0.83	0.53	1.18	1.22	0.80	0.63
Lu	0.12	0.08	0.17	0.18	0.12	0.09
Hf	1.16	0.82	1.41	1.87	1.04	0.94
Ta	0.19	0.14	0.21	0.33	0.14	0.16
Pb	3.06	1.29	3.79	6.56	1.85	5.28
Th	1.40	1.02	1.81	2.69	1.23	1.18
U	0.41	0.28	0.52	0.79	0.35	0.41
Calculated values						
Eu*	1.07	1.35	0.90	0.96	1.01	1.19
Sr*	1.75	3.61	0.46	1.74	1.54	4.17

value, indicating that there was significant Mg-Fe exchange between olivine and the crystallizing melt during cooling.

The back-calculated Mg# of olivine is also very close to that of orthopyroxene, which occurs always as intercumulus phase. This suggests that orthopyroxene originates from the peritectic reaction of Ol + Melt ⇒ Opx with only slight change in Mg# from the reactant olivine to the product orthopyroxene. This conclusion is also supported by the observation that orthopyroxene at the contact to olivine contains spinel inclusions which were most likely included originally in olivine. In rocks with low amounts of cumulus plagioclase (e.g. sample 9), peritectic reactions of olivine with trapped melt to form orthopyroxene and later Ti-pargasite led to a mineral assemblage with more than 90% of mafic phases (ultramafic cumulates).

Trace elements

The REE patterns of the rocks are characterized by enrichment of light-REE (LREE) with respect to heavy-REE (HREE; Fig. 7a). Samples with low amounts of melt and high amounts of plagioclase (17, J3) display a slight positive Eu anomaly due to a positive Eu anomaly in the cumulus plagioclase. However, because the partitioning of Eu plagioclase/melt is <1 (e.g. ~0.1; Bindeman et al. 1998), high amounts of trapped melt prevent an accentuated positive Eu anomaly, which is visible in pure cumulitic gabbros. The sample (9), which does not contain cumulus plagioclase, displays a slight negative Eu anomaly.

The rocks display a strong enrichment of LILE and Pb and to a lesser extent LREE with respect to HREE in a mantle-normalized spidergram of incompatible elements (Fig. 7b). Nb, Ta, and Ti are depleted with respect to neighboring elements with similar chemical characteristics. Sr values change over a factor of 6.5. Sr is compatible in plagioclase (Bindeman et al. 1998) and consequently the positive Sr anomaly is in first approximation a function of the amount of plagioclase (Fig. 6a). Sample (9) is characterized by a negative Sr-anomaly in agreement with a negative Eu anomaly, indicating possible plagioclase fractionation prior to cumulate crystallization.

Despite the strong variation in the amount of cumulus minerals, the incompatible element and REE patterns of the rocks are very similar (Fig. 7). This can be explained by the fact that most of these trace elements do not enter spinel, olivine, or plagioclase and that the patterns are dominated by the trapped melt. In fact, the abundance of trace elements correlates very well with the estimated amount of trapped melt (Fig. 7). The different degree of differentiation is only visible when the HREE content of the melt is recalculated considering its estimated abundance. The Yb_N increases with decreasing Mg# of the melt (Fig. 5a) in agreement with an increasing degree of differentiation.

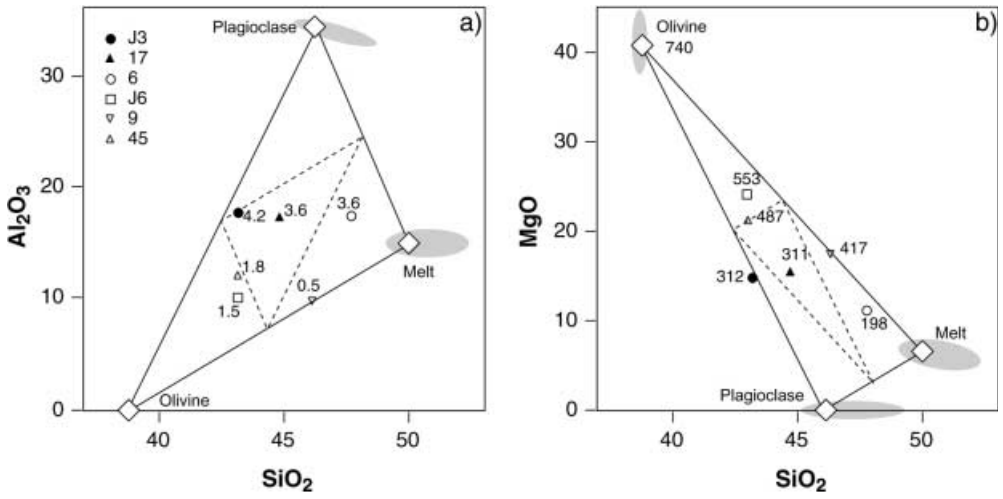

Fig. 6a, b Variation diagrams of major element composition of the mafic-ultramafic cumulates. The compositional ranges of cumulus olivine and plagioclase are given as *gray fields*. The composition of the coexisting melt was considered to be basaltic with representative values of $SiO_2 = 49–52$ wt%, $Al_2O_3 = 14–16$ wt% and $MgO = 6–8$ wt%. For the estimation of modes given in Table 2 an olivine Fo_{80}, a plagioclase An_{84} and a melt with 50% SiO_2, 15% Al_2O_3 and 7% MgO have been chosen. Labels in **a** refer to the Sr* anomaly ($2*Sr_N/Pr_N + Nd_N$) which is a qualitative index for the amount of cumulus plagioclase. Labels in **b** indicate the Ni content of bulk rock, which is a qualitative index for the amount of cumulus olivine. The Ni content of the olivine end-member was obtained from olivine microprobe data (Table 1)

Geochronological data

Mafic-ultramafic cumulate

Zircons have been separated from a sample purposely collected after the geochemical investigations. Despite an absence of geochemical data, this plagioclase-poor cumulate shares the same petrographic features as the samples described above, including a well-preserved magmatic mineralogy with a moderate Alpine overprint. The zircon crystals are clear, colorless and preserve their crystals faces. Their dimension varies between 250 and 100 μm, and they are often fragments of larger crystals. Cathodoluminescence imaging reveals a weak magmatic oscillatory zoning (Fig. 8a), typical of zircon from mafic rocks (Rubatto et al. 1998; Rubatto and Gebauer 2000). In several grains the magmatic zoning is crosscut by domains with chaotic, cloudy zoning and locally surrounded by high luminescent rims, both lacking a regular internal structure (structure-less; Fig. 8a, b). Domains with similar zoning features have been previously described in gabbroic zircon and associated to Pb loss after crystallization (Rubatto et al. 1998).

SHRIMP U-Th-Pb analyses were carried out on both oscillatory-zoned areas (15 analyses) and structure-less domains (7 analyses). All the data appear concordant and mainly cluster at around 300 Ma (Fig. 9a). One analysis for each type of zircon domain is significantly younger and plots off the cluster. These two analyses are suspected to have experienced Pb loss and are excluded from the following calculations. The oscillatory-zoned domains have higher Th/U than the structure-less domains (0.75–4.7 versus 0.12–0.77). They also have ages spanning toward older values (293–327 versus 293–315 Ma) in agreement with the textural relations observed in cathodoluminescence. The cumulative probability curve and the histogram (Fig. 9b) suggest a double distribution of the data with an older group composed mainly of oscillatory zoned domains and a younger group dominated by structure-less domains. The lack of a homogenous population is supported by a MSWD of 6.8 for the cumulative age of the 20 analyses (306 ± 5 Ma). If the data are grouped according to zoning pattern, the oscillatory-zoned domains yield an age of 309 ± 5 Ma (MSWD = 6) and the structure-less domains an age of 298 ± 7 Ma (MSWD = 3). We prefer this grouping of the analyses instead of a single cluster because it is more consistent with cathodoluminescence observations, Th-U data, and geological context. The relatively large spreading of ages in both populations, as indicated by high MSWD, could be either the result of some disturbance of the U-Pb system during a later thermal overprint or an effect of the relatively small number of analyses.

Metagranodiorite

Zircon from a metagranodiorite cropping out near the mafic-ultramafic cumulate has been dated in order to constrain the relative timing of emplacement of cumulates and acid magmas. The dated metagranodiorite displays a slight foliation and consists of quartz, plagioclase (An_{20}), biotite, muscovite and epidote (Cesare et al. 2001).

The zircons from the metagranodiorite show typical granitic features: they are euhedral, elongated, clear, colorless or light pink, and contain rare inclusions. Their maximum dimension is 300 μm. All the crystals preserve a magmatic oscillatory zoning without evidence of inherited cores. A small number of grains have small,

non-zoned areas (≤ 30 μm large) either at the edge of the crystal or around inclusions (Fig. 8c).

The oscillatory-zoned zircons have, with the exception of a dark core, medium U and Th contents and Th/U ratio (0.15–0.60; Table 3). They all yielded concordant ages averaging 295 ± 3 Ma (Fig. 9c). The non-zoned areas of the zircons gave variable ages of between 300 and 20 Ma. Two of these analyses cluster together with the oscillatory-zoned domains, two are slightly but distinctly younger (280 ± 5 and 265 ± 4 Ma, Fig. 9d) and two yielded apparent $^{206}Pb/^{238}U$ ages at around 20 Ma (22 ± 4 and 21 ± 2 Ma). The Alpine domains have U and Th contents, and Th/U ratio much lower than all the other analyses from this sample.

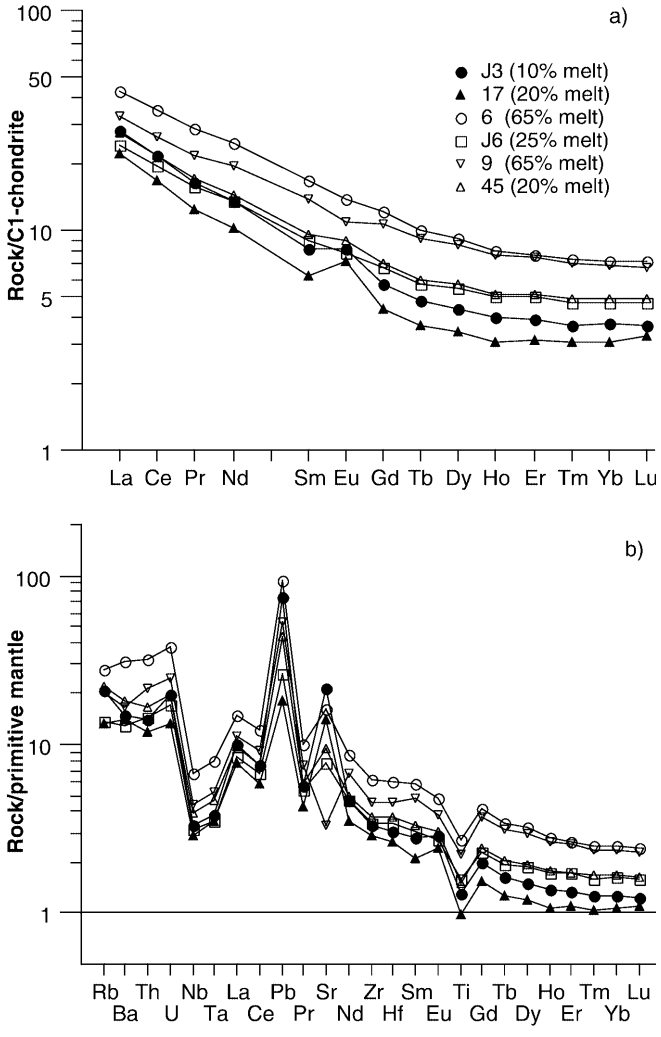

Fig. 7 **a** Chondrite normalised REE patterns and **b** primitive mantle-normalized incompatible element spidergrams of the analyzed samples. Normalization values are taken from Sun and McDounough (1989)

Discussion

Interpretation of U-Pb ages

In the metagranodiorite, the oscillatory-zoned domains have all the characteristic of magmatic zircon: euhedral shape, polygonal oscillatory zoning, medium U and Th contents and medium Th/U ratio. Their age is therefore interpreted as dating the crystallization of the granodiorite at 295 ± 3 Ma. The non-zoned domains crosscut the oscillatory zoning and therefore represent a later event. The scattered ages suggest that these zircon domains underwent a sub-solidus recrystallization process as often described in metamorphic rocks (Rubatto et al. 1999; Hoskin and Black 2000). Such a process erased the oscillatory zoning, induced depletion of U and particularly Th, and produced Pb loss. In particular Pb loss and Th/U ratio are indicative of the amount of recrystallization that affected the zircons. In the 300-Ma-old non-zoned domains the U-Th-Pb system was virtually unaffected by recrystallization. The two youngest domains have very low U contents and Th/U

Fig. 8a–c Cathodoluminescence images of zircon crystals with indicated the SHRIMP pits (diameter~25 μm) and the corresponding $^{206}Pb/^{238}U$ ages (Ma ± 1σ). **a** Zircons from mafic-ultramafic cumulate. In the larger crystal, a light rim with a similar age surrounds the dark, weakly oscillatory-zoned domain. **b** Zircon from the mafic-ultramafic cumulate in which the oscillatory zonation has been almost completely replaced by a chaotic, structure-less pattern. **c** Zircon from metagranodiorite with a magmatic, oscillatory-zoned core surrounded by an non-zoned rim of Alpine age

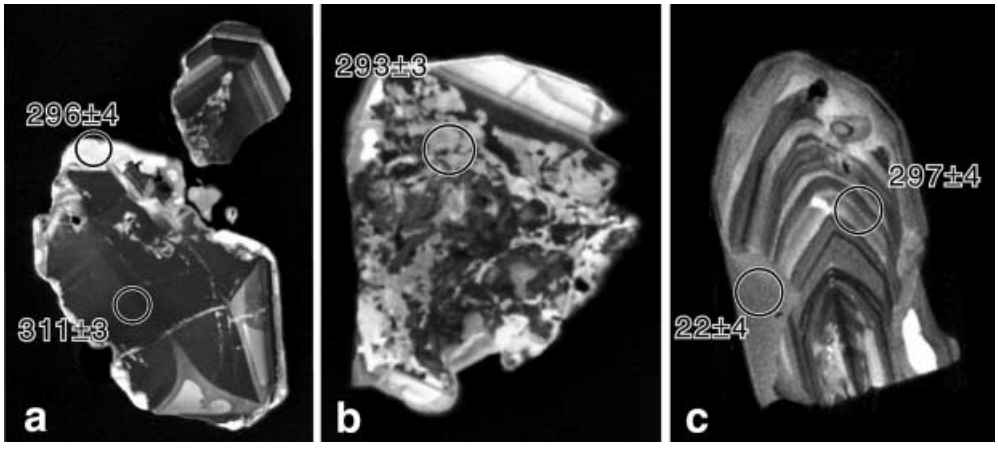

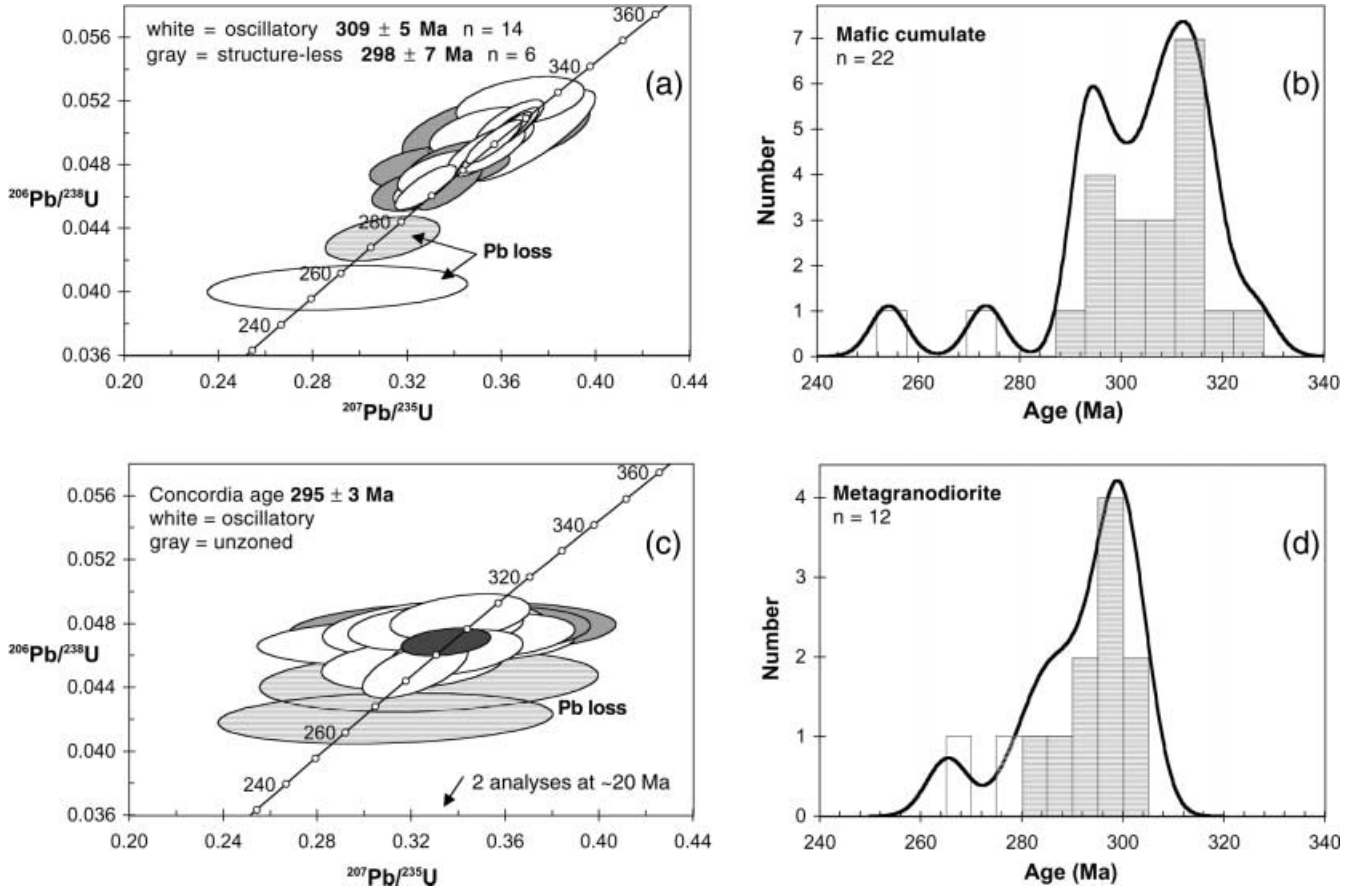

Fig. 9 SHRIMP U-Pb data of mafic-ultramafic cumulate (**a** and **b**) and metagranodiorite, excluding the two youngest data points (**b** and **d**). In the concordia diagrams (**a** and **c**) the error ellipses (2σ) are color-coded according to the zoning pattern of the zircon analyzed. Analyses affected by Pb loss are plotted as semi-transparent ellipses and are excluded from any age calculation. The *dark gray ellipse* in **c** represents the concordia age. Mean ages are given at 95% confidence level. Plots **b** and **d** are histograms with superimposed cumulative probability curves (Ludwig 2000). Analyses affected by Pb loss are *white*. See text for discussion

ratios and are clearly strongly recrystallized. The maximum age for the Alpine metamorphic event inducing recrystallization is thus ~20 Ma. The zircons in the mafic-ultramafic cumulate also appear to have two distinct crystallographic domains: oscillatory zoned and structure-less. As for the granodiorite, the oscillatory-zoned domains are magmatic and date the crystallization of the cumulate at 309 ± 5 Ma.

The structure-less domains cannot be easily attributed to Alpine metamorphism because their ages do not scatter toward 20 Ma, neither is their U content significantly different from the magmatic domains. Instead, the fact that the ages of these domains form a reasonably well-defined cluster is an indication that they date a process that occurred at 298 ± 7 Ma. This age corresponds to the intrusion of the granitic magmas into the cumulate. Such an intrusion could have produced enough heat and fluids to partly recrystallize the magmatic zircons, locally erase their zoning along rims and fractures, and reset their U-Pb system. This process has been described in detail by Pidgeon (1992), who also pointed out that it can occur close to the age of primary crystallization. The high U and Th content of the magmatic zircon might have also assisted recrystallization during contact metamorphism. This event could also be responsible for the excess scatter in the ages of the oscillatory-zoned domains, which have a rather high MSWD of 6. Therefore, the best estimate for the crystallization age of the mafic-ultramafic cumulate is 309 ± 5 Ma. After solidification, the rock was intruded by granodioritic magmas at 295 ± 3 Ma, which produced some recrystallization in the zircon from the cumulate. The relative timing of the two intrusive rocks is supported by the observation that the granodiorite crosscuts the mafic-ultramafic cumulates after their solidification (Fig. 3).

The small difference in age between the cumulate and the granitic magmas reinforces the hypothesis of a genetic link between these two rock types. The cumulate represents the early product of the Late Carboniferous magmatic cycle, which thus started somewhat earlier than previously thought (Eichhorn et al. 2000) and lasted for about 15 Ma. Whereas mafic rocks of Carboniferous age are unknown in the rest of the Tauern window (Finger et al. 1993; Eichhorn et al. 2000), the associated intermediate to acid magmatism is well documented. In the central Tauern window the

Table 3 SHRIMP U-Th-Pb data from zircon of the mafic-ultramafic cumulate (TC) and the metagranodiorite (TG). Errors are quoted at 1σ level. *osc* Oscillatory-zoned; *str* structure-less, i.e. non-zoned or cloudy zoned; *nz* non-zoned; *208* common Pb correction according to ^{208}Pb; *na* not available because the ratio cannot be corrected for common Pb

	U (ppm)	Th (ppm)	Th/U	^{204}Pb/^{206}Pb	^{206}Pb/^{238}U	^{207}Pb/^{235}U	^{207}Pb/^{206}Pb	Age ^{206}Pb/^{238}U
TC-5.1 osc	1,707	1,491	0.87	0.00018	0.04675 ± 62	0.3327 ± 75	0.05161 ± 87	295 ± 4
TC-9.1 osc	780	1,833	2.35	0.00014	0.04960 ± 62	0.3518 ± 91	0.0514 ± 11	312 ± 4
TC-9.2 osc	674	1510	2.24	0.00015	0.05010 ± 63	0.3515 ± 88	0.0509 ± 10	315 ± 4
TC-11.1 osc	1,477	1,973	1.34	0.00006	0.04895 ± 58	0.3511 ± 56	0.05202 ± 48	308 ± 4
TC-13.1 osc	665	1,026	1.54	0.00011	0.04749 ± 57	0.3348 ± 77	0.05113 ± 93	299 ± 3
TC-17.1 osc	2,326	2,977	1.28	0.00005	0.05060 ± 60	0.3639 ± 60	0.05215 ± 52	318 ± 4
TC-19.2 osc	5,298	4,875	0.92	0.00013	0.04654 ± 58	0.3281 ± 54	0.05113 ± 47	293 ± 4
TC-20.1 osc	5,795	1,2663	2.19	0.00005	0.05196 ± 65	0.368 ± 11	0.0514 ± 14	327 ± 4
TC-22.2 osc	4,692	10,864	2.32	0.00028	0.04022 ± 57	0.291 ± 23	0.0524 ± 39	254 ± 4
TC-23.1 osc	3,289	2,875	0.87	0.00002	0.04990 ± 58	0.3614 ± 48	0.05252 ± 28	314 ± 4
TC-24.2 osc	2,751	7,714	2.80	0.00004	0.04887 ± 55	0.3569 ± 55	0.05297 ± 48	308 ± 3
TC-25.1 osc	2,138	1,610	0.75	0.00001	0.04945 ± 56	0.3572 ± 49	0.05238 ± 34	311 ± 3
TC-26.1 osc	1,617	7,722	4.77	0.00001	0.0499 ± 12	0.373 ± 11	0.05420 ± 89	314 ± 7
TC-30.1 osc	2,364	2,602	1.10	0.00003	0.04872 ± 60	0.3541 ± 53	0.05272 ± 37	307 ± 4
TC-32.1 osc	4,146	6,310	1.52	0.00003	0.05019 ± 58	0.3640 ± 50	0.05261 ± 33	316 ± 4
TC-4.1 str	1,267	103	0.08	0.00001	0.04656 ± 58	0.3382 ± 57	0.05268 ± 53	293 ± 4
TC-21.1 str	3,083	2,376	0.77	0.00010	0.0501 ± 10	0.358 ± 16	0.0518 ± 20	315 ± 6
TC-22.1 str	1,500	1,201	0.80	0.00011	0.04645 ± 57	0.3266 ± 88	0.0510 ± 12	293 ± 3
TC-24.1 str	1,121	135	0.12	0.00011	0.04802 ± 59	0.3386 ± 77	0.05115 ± 90	302 ± 4
TC-25.2 str	1,613	527	0.33	0.00004	0.04676 ± 62	0.3360 ± 64	0.05211 ± 62	295 ± 4
TC-31.1 str	1,618	623	0.39	0.00027	0.04332 ± 57	0.3097 ± 99	0.0519 ± 14	273 ± 4
TG-2.1 osc	287	116	0.40	0.00030	0.04718 ± 60	0.351 ± 16	0.0539 ± 23	297 ± 4
TG-3.1 osc	513	302	0.59	0.00031	0.04618 ± 58	0.340 ± 11	0.0533 ± 16	291 ± 5
TG-5.1 osc	608	308	0.51	0.00029	0.04840 ± 60	0.341 ± 12	0.0511 ± 16	305 ± 4
TG-6.1 osc	402	190	0.47	0.00044	0.04542 ± 64	0.321 ± 16	0.0512 ± 24	286 ± 4
TG-8.1 osc	286	102	0.36	0.00057	0.04763 ± 72	0.330 ± 19	0.0502 ± 28	300 ± 4
TG-9.1 osc	321	126	0.39	0.00083	0.04681 ± 63	0.322 ± 28	0.0499 ± 42	295 ± 4
TG-10.1 osc	4,598	1,207	0.26	0.00018	0.04509 ± 74	0.3220 ± 92	0.0518 ± 11	284 ± 5
TG-11.1 osc	273	102	0.38	0.00062	0.04774 ± 61	0.330 ± 15	0.0502 ± 22	301 ± 4
TG-1.1 nz	218	43	0.20	0.00040	0.04749 ± 66	0.344 ± 22	0.0525 ± 31	299 ± 4
TG-2.2^{208} nz	17	0.03	0.002	0.04586	0.00349 ± 55	0.079 ± 50	na	22 ± 4
TG-4.1 nz	198	27	0.14	0.00087	0.04203 ± 66	0.309 ± 29	0.0534 ± 49	265 ± 4
TG-6.2^{208} nz	16	0.08	0.005	0.03686	0.00324 ± 33	na	na	21 ± 2
TG-7.1 nz	145	32	0.22	0.00111	0.04435 ± 79	0.328 ± 30	0.0536 ± 46	280 ± 5
TG-12.1 nz	225	35	0.15	0.00058	0.04763 ± 69	0.338 ± 29	0.0514 ± 42	300 ± 4

Venediger tonalite intruded at 296 ± 4 Ma (Eichhorn et al. 2000) and a tonalitic pluton has been dated at 314 ± 7 Ma in the southeast (Cliff 1981). This Late Carboniferous subduction-related magmatism can thus be tracked over a large part of the Tauern window.

In the Central and Western Alps Late Carboniferous mafic magmatism remains virtually unknown or undetected. As in the Tauern window, the main magmatic pulse documented in the 310–295 Ma period is acidic in composition (see Debon and Lemmet 1999 for a review). The only exceptions are rare gabbroic enclaves (~307 Ma, Bussy and Hernandez 1997) and some high-K intermediate sills (310 ± 3 Ma, Schaltegger and Corfu 1995).

On the other hand, mafic magmatism is well documented for the period immediately before and after the formation of the Tauern window cumulates. A high-Mg suite with intermediate and basic members of Visean age (~340 Ma) was defined by Debon and Lemmet (1999) for the external massifs of the Central and Western Alps. Subordinate mafic rocks with an age of 330–340 Ma are present in the Bernina calk-alkaline intrusion suite (Büchi 1994; von Quadt et al. 1994). Gabbroic magmas form large parts of the Permian bimodal magmatic cycle dated at around 290–275 Ma. This Permian mafic magmatism is present mainly along the internal region of the Alpine chain and in the Southern Alps (Hermann et al. 1997; Rubatto et al. 1999; Tribuzio et al. 1999; Mayer et al. 2000) and is also documented in the Eastern Alps (Thöni and Jagoutz 1992; Miller and Thöni 1997). The chemical character of the Permian mafic magmatism is tholeiitic (e.g. Voshage et al. 1990; Tribuzio et al. 1999; Hermann et al. 2001).

Origin of mafic-ultramafic cumulates

Evidence for subduction-type magmatism

There are several lines of evidence indicating that the mafic-ultramafic cumulates are related to subduction-type magmatism.

Field relations and SHRIMP data indicate that the mafic-ultramafic cumulates formed prior to the tonalite-

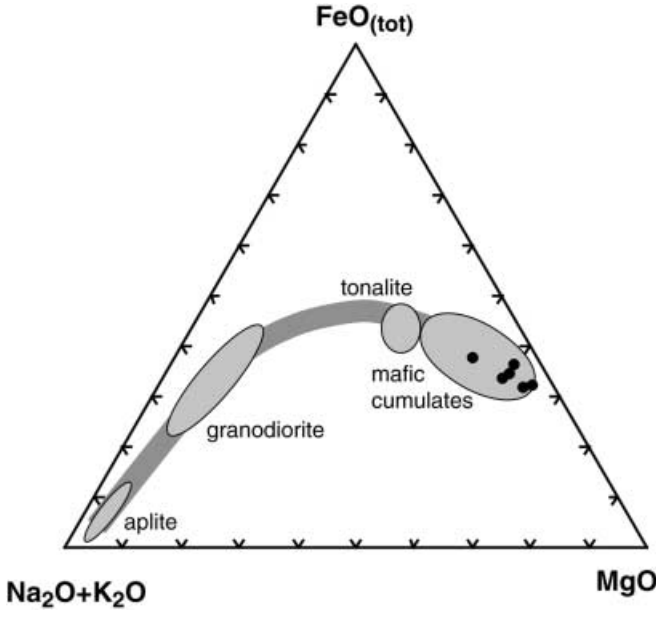

Fig. 10 Evolution trend in the AFM diagram of plutonic rocks from the northwestern part of the Central Gneiss (Berliner Hütte) after Wyss (1993). The mafic-ultramafic cumulates described in this paper are shown as *black dots* and represent the most primitive members of the rock suite

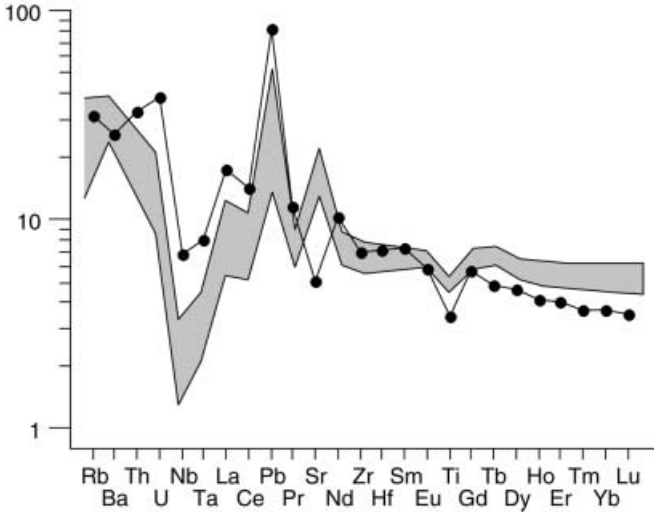

Fig. 11 The recalculated trace element pattern of the parental melt of the most primitive sample 9 (*black dots*) is very similar to the compositional range of primitive arc lavas from the Mariana subduction zone (*gray field* after Elliott et al. 1997). See text for discussion

granodiorite suite. The age of the cumulate is only slightly older than the age of the adjacent metagranodiorite, indicating that both rock types were produced during the same geologic event. This is in agreement with field evidence reported by Wyss (1993) and Frasl and Schindlmayr (1995) who suggested that mafic to ultramafic cumulates and enclaves in the tonalite are co-genetic. The whole range of different rock types in the Zillertal massif have been analyzed by Wyss (1993) and describe a "calc-alkaline" trend in the AFM diagram (Fig. 10). The mafic-ultramafic cumulates studied here overlap with the completely amphibolitized cumulates reported by Wyss (1993). Therefore, we interpret the cumulate as the most primitive preserved member of a subduction-related magmatic suite that includes the granodiorites and tonalites.

The trace element contents of the rocks display all major features of subduction zone magmas: strong enrichment in LILE and Pb; slight enrichment in LREE with respect to HREE; relative depletion of Nb, Ta, and Ti (Perfit et al. 1980; Tatsumi and Eggins 1995).

For the first time we report the composition of preserved magmatic minerals from mafic-ultramafic cumulates of the Zillertal massif. Primitive arc rocks are characterized by high An contents in plagioclase, which is caused by relatively high water contents in the melt. The high An content of plagioclase and the intermediate to high Mg# of coexisting olivine in the investigated cumulates are in agreement with formation from subduction zone magmas. In contrast, tholeiitic mafic rocks such as the Sondalo troctolites (Tribuzio et al. 1999) or the Malenco olivine–gabbronorites (Hermann et al. 2001) contain plagioclase with significantly lower An-contents (Fig. 5b).

Parental melt

Cumulate 9 is the best sample to infer the composition of the parental magma of the mafic-ultramafic cumulates because it has the highest Mg# of the original olivine (Fig. 6), a high percentage of trapped melt and contains no cumulus plagioclase, which could affect the recalculation of LILE. The mass balance indicates that this sample represents about 35% of cumulus olivine with minor Cr-spinel inclusions and 65% of trapped melt. Because olivine and Cr-spinel do not incorporate significant incompatible trace elements, their amount in the melt can be directly recalculated from mass balance (Fig. 11). The resulting pattern is very similar to the range of primitive lavas from the Mariana arc (Eliott et al. 1997) and demonstrates a subduction-type origin of the parental melt of the mafic-ultramafic cumulates (Fig. 11). The most significant difference is the negative Sr-anomaly of the parental melt. Because Sr is compatible in plagioclase (Bindeman 1998), early plagioclase fractionation might result in a negative Sr-anomaly in the residual melt. Thus, a possible explanation for negative Sr and Eu anomalies is that significant plagioclase fractionation occurred at greater depth where the crystallization was dominated by olivine + pyroxene + plagioclase. A previous fractional crystallization of Mg-Fe phases is supported also by the Mg# of the rocks. The most primitive recalculated Mg# of cumulus olivine is 0.84, which is significantly lower than Mg# of 0.90 which forms from non-fractionated primitive arc magmas.

Conditions of intrusion

The observed crystallization sequence and the chemical information gathered on the mineral assemblage help to constrain the conditions of intrusion of the mafic-ultramafic cumulates. The temperature of the magma at the time of intrusion can be estimated on the basis of the most primitive recalculated olivine (Fo_{84}). Assuming a likely MgO content of 6–8% in the parental basaltic liquid (see Fig. 5), a crystallizing olivine with Fo_{84} indicates temperatures of $1{,}050 \pm 50$ °C according to the experiments of Roeder and Emslie (1970). In order to obtain such low temperatures at the basalt liquidus, a significant amount of H_2O of 5–6 wt% is necessary (Green 1982). An important consequence of a high water content is that the plagioclase stability field in P–T space moves to lower pressures. In the studied rocks, plagioclase is a cumulus phase crystallizing after olivine but prior to pyroxene. This is only possible at pressures below 3 kbar (Green 1982). The two constraints, H_2O contents of 5–6 wt% and low pressure crystallization, permit comparison of the mafic rocks with low pressure, water saturated experiments of Moore and Carmichel (1998) on a basaltic-andesitic composition (Fig. 12). At about 2 kbar, most of the features of the mafic-ultramafic cumulates are met. The melt contains about 4.5 wt% of H_2O and the temperature of first olivine crystallization is about 1,070 °C. The crystallization sequence is Cr-spinel > Ol > Plag in agreement with the observed sequence in the cumulates. Interestingly, no magmatic clinopyroxene has been observed. This could be explained by the formation of Ca-rich plagioclase resulting in a residual melt with low Ca activity and the crystallization of intercumulus orthopyroxene. At pressures higher than 2 kbar, phase relationships change in a way that amphibole should crystallize as a cumulus phase instead of plagioclase at high H_2O activity. At lower pressures, the liquidus temperature is significantly higher. The anorthite content of plagioclase increases with increasing T and increasing water pressure, and provides additional information on the formation conditions. Plagioclase with An_{80} forms at 1,000° C and 2 kbar H_2O pressure (Housh and Luhr 1991; Moore and Carmichel 1998). The agreement of experimental data with the observed crystallization sequence and the chemical composition of cumulus minerals indicates that the temperature of the parental magma was about 1,050–1,100° C and the depth of intrusion was approximately 7 km. A shallow level of intrusion has been also proposed from field relations (Finger et al. 1993) and geochronology, which indicates a period of exhumation prior to the formation of the Venediger massif (Eichhorn et al. 2000).

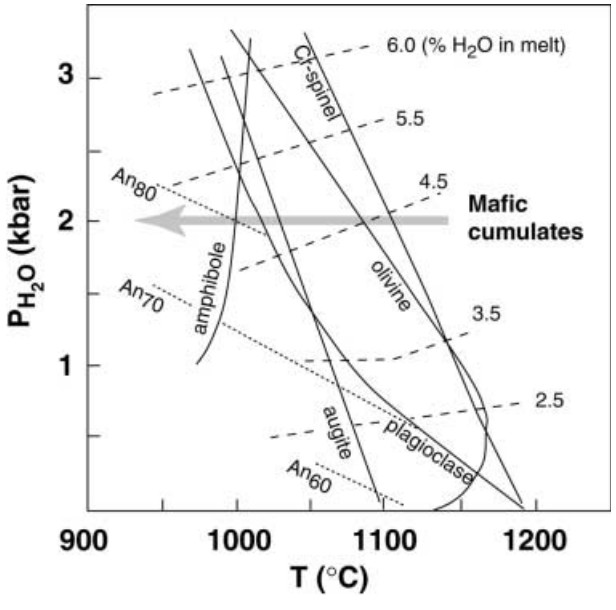

Fig. 12 Schematic pressure–temperature diagram of phase relations in a H_2O-saturated basaltic andesite after Moore and Carmichael (1998). The first occurrences of phases are shown with *solid lines*. Contours of H_2O contents in melts are indicated by *dashed lines* and contours of anorthite contents in plagioclase are shown by *dotted lines*. The observed features in the cumulates suggest crystallization at ~2 kbar

Geological significance of the mafic-ultramafic cumulates

Field evidence, geochemistry, and age determinations have demonstrated that the mafic-ultramafic cumulates are the most primitive members of a subduction-type magmatism in the Zillertal massif. The most primitive recalculated olivine Mg# of 0.84 indicates that the parental melt had already differentiated at greater depth, most probably at lower crustal levels. This is in agreement with the slight negative Sr anomaly of the parental melt (Fig. 11) which argues for fractionation of some plagioclase prior to the emplacement of mafic melts. Based on field relations, it has been proposed that basaltic-andesitic dikes occasionally crosscut the still hot tonalite (Wyss 1993; Frasl and Schindlmayr 1995). This observation supports the existence of a deep-seated magma chamber in which differentiation/assimilation took place and from which magmas escaped at different stages of their evolution. The crystallization sequence in the mafic-ultramafic cumulates indicates intrusion at shallow crustal levels of about 7 km. Consequently, the small volumetric ratio of mafic rocks to granitoids (Fig. 2) should not be regarded as representative for the whole magmatic activity. Because mafic melts are much denser than hydrous granitic melts, large volumes of mafic rocks might have intruded at mid- to lower crustal levels. The estimated temperature of 1,050–1,100 °C for the parental melt of the mafic-ultramafic cumulates provides a minimum temperature for mafic intrusions at depth. Such hot mafic intrusions can produce considerable partial melting in and assimilation of lower crustal rocks. A differentiation/assimilation process in the lower crust is in line with isotope data from the tonalite, which point to a mixed crustal and mantle source for the tonalite magmas

(Finger et al. 1993; Finger 1997). Combined with age data of the more evolved intrusives, the new age data on the mafic-ultramafic cumulates permit one to estimate a time span of magmatic activity from 310 to 295 Ma. It is not yet clear, if this time span represents a continuous magmatic evolution or a sporadic refill of the deep-seated magma chamber by mantle melts, followed by extraction of differently evolved magmas to upper crustal levels.

Recent SHRIMP dating of the central Tauern window rock suites has revealed a multistage Variscan magmatic evolution (Eichhorn et al. 2000). Subduction-related magmatism (~375 Ma) at an initial stage of convergence is followed by collision-type magmatic activity (345–335 Ma), which mainly consists of anatectic crustal melts. A period of quiescence and exhumation is followed by the emplacement of I-type Venediger tonalite and related rocks in the time span of 300–295 Ma. Our data permit us to trace back the beginning of this event to 310 Ma and to define the source of the magmas. The youngest magmatic event documented in the Tauern window consists of S-type granites, which were emplaced at 280–270 Ma.

Two main models have been suggested to explain the 310–295 Ma I-type magmatism: (1) intracontinental extension associated with minor decompression and mantle melting, unrelated to subduction (Schaltegger and Corfu 1995; Schaltegger 1997; Eichhorn et al. 2000); (2) subduction zone magmatism in an active continental margin setting (Finger and Steyrer 1990). The chemical and mineralogical data reported in this paper provide evidence that subduction-type magmatism with mantle-derived melts was involved in the formation of the Zillertal massif. This observation creates an apparently tectono-magmatic enigma because this subduction-type magmatism occurs between Carboniferous syn- to post-orogenic anatectic magmatic activity (Finger 1997; von Raumer 1998) and Permian large-scale tholeiitic magmatic activity (Voshage et al. 1990; Tribuzio et al. 1999; Hermann et al. 2001). Finger and Steyrer (1990) suggested that continuous subduction of the paleo-Tethys was the cause of I-type magmatism in the Tauern window. The detailed age determinations of Eichhorn et al. (2000) do not support this hypothesis because there is a period of quiescence prior to the formation of the Venediger massif rather than continuous I-type magmatic activity. Additionally, paleogeographic reconstruction indicates that within the "Alpine terrane" the Tauern window plutons were about 250 km away from the estimated locus of active subduction (Stampfli 1996; von Raumer 1998; Eichhorn et al. 2000). An alternative hypothesis to explain the subduction-type magmatism, recently put forward by Finger et al. (1997), includes slab break off during ongoing convergence. Slab break off of ancient subducted oceanic crust would lead to a temperature rise and to local production of subduction-type magmatism (von Blankenburg and Davies 1995). In areas where the mantle has not been metasomatized by subduction zone fluids, mantle upwelling would produce more alkaline magmas as observed in the Bernina Massif (Büchi 1994) and could lead to magmatism associated with minor mantle components in an intracontinental extensional setting (Schaltegger and Corfu1995, Schaltegger1997). Delamination of the lithosphere by slab break off could also be regarded as an initial stage of the Permian tholeiitic magmatism, which produced huge amounts of mafic melts by decompression melting of mantle rocks. In such a scenario the Late Carboniferous subduction-type magmatism documented in the studied cumulates would represent a logic continuum from the Variscan syn- to post-collisional magmatism to the Permian extensional magmatism rather than an isolated reactivation of subduction of oceanic crust.

Concluding remarks

The mafic-ultramafic cumulates found in the Zillertal massif testify for an early phase of the Late Carboniferous calc-alkaline plutonic activity in the SW Tauern window. This activity, recently restricted to the Stephanian (Eichhorn et al. 2000), is here traced back to the Westphalian (309 ± 5 Ma), approximately 10 Ma before the emplacement of the main granodioritic to tonalitic intrusions (295 ± 3 Ma).

Petrology and geochemistry of the fresh mafic-ultramafic cumulates reveal that they originated from mafic melts, which underwent minor differentiation at lower-middle crustal levels. These cumulates are proof of the involvement of mantle derived melts in the formation of the Central Gneiss. To explain the characteristic subduction-type signature of the parental melt of the cumulates, we propose that the magmatism was caused by a slab of ancient subducted oceanic crust breaking off during ongoing convergence between the paleo-Tethys and the Alpine terrane.

Acknowledgements Many thanks to S. Meli, E. Poletti and S. Jap for support during fieldwork, to G. De Vecchi, F. Finger and B. Lammerer for kindly providing unpublished data and information, to A.M. Fioretti and A. Jama Aden for discussion and comments, and to F. Finger and R. Eichhorn for their helpful reviews of the manuscript. The Electron Microscope Unit at the Australian National University is thanked for access to SEM facilities. Financial support to B.C. from Università di Padova (Fondi Progetti di Ricerca 1998) and Consiglio Nazionale delle Ricerche (CSGA, Padova) is gratefully acknowledged.

References

Arming W (1993) Zur Geologie und Petrographie der dunklen Einschlussmassen im Zentralgneisgebiet des Zillertal-Venediger-Kerns. Diploma Thesis, Univ Salzburg

Barzi L (1996) Studio petrografico di cumulati ultrabasici e basici a sud-est della Cima di Campo–Turnerkamp (Alti Tauri–Alto Adige). Diploma Thesis, Univ Padova

Bindeman IL, Davis AM, Drake MJ (1998) Ion microprobe study of plagioclase-basalt partition experiments at natural concentration levels of trace elements. Geochim Cosmochim Acta 62:1175–1193

Büchi HJ (1994) Variscan magmatism in the eastern Bernina area (Grisons, Switzerland). Schweiz Mineral Petrol Mitt 74:359–371
Bussy F, Hernandez J (1997) Short-lived bimodal magmatism at 307my in the Mont-Blanc/Aiguilles-Rouges area: a combination of decompressional melting, basaltic underplating and crustal fracturing. Quad Geodin Alpina Quat 4:22
Cesare B, Poletti E, Boiron M-C, Cathelineau, M (2001) Alpine metamorphism and veining in the Zentralgneis Complex of the SW Tauern window: a model of fluid-rock interactions based on fluid inclusions. Tectonophysics 336:121–136
Christensen JN, Selverstone J, Rosenfeld JL, DePaolo DJ (1994) Correlation by Rb-Sr geochronology of garnet growth histories from different structural levels within the Tauern window, Eastern Alps. Contrib Mineral Petrol 118:1–12
Cliff RA (1981) Pre-Alpine history of the Penninic zone in the Tauern window, Austria: U-Pb and Rb-Sr geochronology. Contrib Mineral Petrol 77:262–266
Compston W, Williams IS, Kirschvink JL, Zhang Z, Ma G (1992) Zircon U-Pb ages for the Early Cambrian time-scale. J Geol Soc Lond 149:171–184
De Vecchi GP, Baggio P (1982) The Pennine Zone of the Vizze region in the western Tauern window (Italian eastern Alps). Boll Soc Geol It 101:89–116
De Vecchi GP, Mezzacasa G (1986) The Pennine Basement and cover units in the Mesule group (Southwestern Tauern window). Mem Sci Geol 38:365–392
Debon F, Lemmet M (1999) Evolution of Mg/Fe ratios in the Late Variscan plutonic rocks from the External Crystalline Massifs of the Alps (France, Italy, Switzerland). J Petrol 40:1151–1185
Eggins SM, Rudnick RL, McDonough WF (1998) The composition of peridotites and their minerals: a laser ablation ICP-MS study. Earth Planet Sci Lett 154:53–71
Eichhorn R, Loth G, Höll R, Finger F, Schermaier A, Kennedy A. (2000) Multistage Variscan magmatism in the central Tauern window (Austria) unveiled by U/Pb SHRIMP zircon data. Contrib Mineral Petrol 139:418–435
Ernst WG (1978) Petrochemical study of lherzolitic rocks from the western Alps. J Petrol 19:341–392
Elliott T, Plank T, Zindler A, White W, Bourdon B (1997) Element transport from slab to volcanic front at the Mariana arc. J Geophys Res 102: 14991–15019
Finger F, Steyrer HP (1988) Granite-types in the Hohe Tauern (Eastern Alps, Austria) – some aspects on their correlation to Variscan plate tectonic processes. Geodyn Acta 2:75–87
Finger F, Steyrer HP (1990) I-type granitoids as indicators of a late Paleozoic convergent ocean-continent margin along the southern flank of the central European Variscan Orogen. Geology 18:1207–1210
Finger F, Frasl G, Haunschmid B, Lettner H, von Quadt A., Schermaier A, Schindlmayr AO, Steyrer HP (1993) The Zentralgneise of the Tauern window (Eastern Alps): insight into an intra-alpine Variscan batholith. In: von Raumer JF, Neubauer F (eds) Pre-Mesozoic geology in the Alps. Springer, Berlin, Heidelberg, New York, pp 375–391
Finger F, Roberts MP, Haunschmid B, Schermaier A, Steyrer HP (1997) Variscan granitoids of central Europe: their typology, potential sources and tectonothermal relations. Mineral Petrol 61: 67–96
Frasl G, Schindlmayr AO (1995) Strukturell gut erhaltene 2-Magmen-Gaenge sowie mafische Enklaven und Grosskoerper in den Zentralgneisen des Zillertal – Venediger- Kerns. Geol Palaeontol Mitt Innsbruck 20:121–151
Friedrichsen H, Morteani G (1979) Oxygen and hydrogen isotope studies on minerals from alpine fissures and their gneissic host rocks, western Tauern window (Austria). Contrib Mineral Petrol 70:149–152
Green TH (1982) Anatexis of mafic crust and high pressure crystallization of andesites. In: Thorpe RS (ed) Andesites. pp 465–487
Hermann J, Müntener O, Trommsdorff V, Hansmann W, Piccardo GB (1997) Fossil crust to mantle transition, Val Malenco (Italian Alps). J Geophys Res 102: 20.123–20.132
Hermann J, Müntener O, Günther D (2001) Differentiation of mafic magma in a continental crust-to-mantle transition zone. J Petrol 42:189–206
Hoernes S, Friedrichsen H (1974) Oxygen isotope studies on metamorphic rocks of the western Hohe Tauern area (Austria). Schweiz Mineral Petrol Mitt 54:769–788
Hoskin PWO, Black LP (2000) Metamorphic zircon formation by solid-state recrystallization of protolithic igneous zircon. J Metamorph Geol 18:423–439
Housh TB, Luhr JF (1991) Plagioclase-melt equilibria in hydrous systems. Am Mineral 76:477–492
Irvine TN (1982) Terminology for layered intrusions. J Petrol 23:127–162
Lammerer B, Weger M (1998) Footwall uplift in an orogenic wedge: the Tauern window in the Eastern Alps of Europe. Tectonophysics 285:213–230
Leake BE (1978) Nomenclature of amphiboles. Am Mineral 63:1023–1053
Ludwig KR (2000) Isoplot/Ex version 2.4. A geochronological toolkit for Microsoft Excel, Berkeley Geochron Centre Spec Publ 1–56
Mayer A, Mezger K, Sinigoi S (2000) New Sm-Nd ages for the Ivrea-Verbano Zone, Sesia and Sessera valleys (northern-Italy). J Geodyn 30:147–166
Miller C, Thoeni M (1997) Eo-Alpine eclogitisation of Permian MORB-type gabbros in the Koralpe (Eastern Alps, Austria): new geochronological, geochemical and petrological data. Chem Geol 137:283–310
Moore G, Carmichael ISE (1998) The hydrous phase equilibria (to 3 kbar) of an andesite and basaltic andesite from western Mexico: constraints on water content and conditions of phenocryst growth. Contrib Mineral Petrol 130:304–319
Morteani G (1974) Petrology of Tauern window, Austrian Alps. Fortschr Miner 52:195–220
Perfit MR, Gust DA, Bence AE, Arculus RJ, Taylor SR (1980) Chemical characteristics of island-arc basalts: implications for mantle sources. Chem Geol 30:227–256
Pidgeon RT (1992) Recrystallisation of oscillatory zoned zircon: some geochronological and petrological implications. Contrib Mineral Petrol 110:463–472
Raith M. (1971) Seriengliederung und Metamorphose im Östlichen Zillertaler Hauptkamm (Tirol/Österreich). Verh Geol Bund 1:163–207
Raith M, Raase P, Kreuzer H, Müller P (1978) The age of the Alpidic metamorphism in the Tauern window, Austrian Alps, according to radiometric dating. In: Closs H, Roedder D, Schmidt K (eds) Alps, Apennines, Hellenides. Inter Union Comm Geodyn Sci Rep 38:140–148
Roeder PL, Emslie RF (1970) Olivine-liquid equilibrium. Contrib Mineral Petrol 29:275–289
Rubatto D, Gebauer D, Fanning M (1998) Jurassic formation and Eocene subduction of the Zermatt–Saas-Fee ophiolites: implications for the geodynamic evolution of the Central and Western Alps. Contrib Mineral Petrol 132:269–287
Rubatto D, Gebauer D, Compagnoni R (1999) Dating of eclogite-facies zircons: the age of Alpine metamorphism in the Sesia-Lanzo Zone (Western Alps). Earth Planet Sci Lett 167:141–158
Rubatto D, Gebauer D (2000) Use of cathodoluminescence for U-Pb zircon dating by ion microprobe: some examples from the Western Alps. In: Pagel M, Barbin V, Blanc P, Ohnenstetter D (eds) Cathodoluminescence in geosciences. Springer, Berlin Heidelberg New York, pp 373–400
Schaltegger U (1997) Magma pulses in the central Variscan belt: episodic melt generation and emplacement during lithospheric thinning. Terra Nova 9 (5-6):242–245
Schaltegger U, Corfu F (1995) Late Variscan "Basin and Range" magmatism and tectonics in the Central Alps: evidence from U-Pb geochronology. Geodin Acta 8:82–98
Selverstone J (1985) Petrologic constraints on imbrication, metamorphism and uplift in the Tauern window, eastern Alps. Tectonics 4:687–704

Selverstone J, Spear FS, Franz G, Morteani G (1984) High pressure metamorphism in the S-W Tauern window, Austria: P–T paths from horneblende–kyanite–staurolite schists. J Petrol 25:501–531

Stampfli GM (1996) The intra-Alpine terrain: a Paleotethyan remnant in the Alpine Variscides. Eclogae Geol Helv 89:13–42

Sun SS, McDonough WF (1989) Chemical and isotope systematics of oceanic basalts: implications for mantle composition and processes. In: Saunders AD, Norry MJ (ed) Magmatism in the ocean basins. Geol Soc Spec Publ 42:313–345.

Thöni M, Jagoutz E (1992) Some new aspects of dating eclogites in orogenic belts: Sm-Nd, Rb-Sr, and Pb-Pb isotopic results from the Austroalpine Saualpe and Koralpe type-locality (Carinthia/Styria, southern Austria). Geochim Cosmochim Acta 56:347–368

Tribuzio R, Thirlwall MF, Messiga B (1999) Petrology, mineral and isotope geochemistry of the Sondalo gabbroic complex (central Alps, northern Italy): implications for the origin of post-Variscan magmatism. Contrib Mineral Petrol 136:48–62

Tatsumi Y, Eggins SM (1995) Subduction zone magmatism. Blackwell, Cambridge, 211 pp

von Blanckenburg F, Davies JH (1995) Slab break-off: a model for syncollisional magmatism and tectonics in the Alps. Tectonics 14:120–131

von Quadt A, Grünenfelder M, Büchi HJ (1994) U-Pb zircon ages from different igneous rocks of the Bernina nappe system (Grisons, Switzerland). Schweiz Mineral Petrogr Mitt 74: 373–382

von Raumer JF (1998) The Paleozoic evolution in the Alps: from Gondwana to Pangea. Geol Rundsch 87:407–435

Voshage H, Hofmann AW, Mazzucchelli M, Rivalenti G, Sinigoi S, Raczek I. Demarchi G (1990). Isotopic evidence from the Ivrea zone for a hybrid lower crust formed by magmatic underplating. Nature 347:731–736.

Wyss M (1993) The migmatite belt at the northern boundary of the Zillertal core of the Tauern Zentralgneisses: a typical intrusive border zone. Schweiz Mineral Petrogr Mitt 73: 435–454